Open charm production at HERA

Ignacio Redondo
on behalf of the H1 and ZEUS Collaborations
Dept. de Física Teórica, Universidad Autónoma de Madrid, Cantoblanco, Madrid 28049, SPAIN
E-mail: redondo@mail.desy.de

Abstract. Measurements of charmed particle cross sections at HERA in the photoproduction and deep inelastic regimes are reviewed. The status of the comparison with perturbative QCD calculations is discussed.

1. Introduction

Open charm production at HERA has developed as a precision testing ground for fixed order (FO) NLO pQCD calculations as well as for other QCD inspired models. The bulk of the available data is on inclusive charmed particle production cross sections for several species. I will focus on reviewing the status of the comparison of the data with FO NLO pQCD calculations trying to identify the open issues for HERA Run II. The description of the kinematics for these observables requires two variables for the charmed particle momentum (an integration over the azimuthal angle of the charmed particle is generally assumed) and one (W) or two (Q^2 and y, for instance) additional variables needed for the description of the inclusive photoproduction (PHP) or deep inelastic (DIS) cross section, respectively. The pseudorapidity, $\eta = -log(tan(\theta/2))$, where θ is the polar angle with respect to the proton (p) direction, and the transverse momentum with respect to the beam line, p_{T}, are typically chosen as the charmed particle variables. Open charm production is intimately related to the gluon parton density in the p because the Photon-Gluon Fusion (PGF) process, sketched in Figure 1 (a), is expected to be one of the dominant production mechanisms. Since the invariant mass of the partonic final state, M^2_{hard}, is significant due to the presence of two heavy quarks ($M^2_{hard} > 4m_c^2$), the kinematics are such that the fraction of the p momentum carried by the gluon $x_g = x_{Bj}(M^2_{hard}+Q^2)/Q^2$ rather than equal to x_{Bj}, as in the quark parton model (QPM) type of process. The sensitivity to the gluon density, f_g, and to α_s can be read from the factorization formula for the PGF process written in equation (1), where $\hat{\sigma}$ is the calculable partonic cross section.

$$\sigma^{c\bar{c}}(x_{Bj},Q^2) \propto e_c^2\alpha_s(\mu_r)\int_{x_g^{min}}^1 \frac{dx_g}{x_g} f_g(x_g,\mu_f)\hat{\sigma}(x_g,\mu_f,\mu_r) \quad ; \quad x_g^{min} = x_{Bj}\frac{4m_c^2+Q^2}{Q^2} \qquad (1)$$

Higher order corrections and the fact that the cross section is measured in restricted regions of the charmed particle phase space complicate this simple picture.

HERA Run I is already finished but the full data samples are just beginning to be exploited. H1 and ZEUS have collected $\gtrsim$ 100 pb^{-1}. This luminosity allows for the selection of large charm samples. This is illustrated in Figure 1 (c), from [1], where $\sim$ 27000 D^* mesons were reconstructed via the widely used K2π, $D^{*+} \to (D^0 \to K^-\pi^+)\pi^+(+\text{c.c.})$, decay channel [2, 3, 4, 5, 6, 7, 8]. This decay mode has a low combinatorial background and a sizable branching ratio (0.0262$\pm$0.0010). D^* mesons have been tagged also via the K4π, $D^{*+} \to (D^0 \to K^-\pi^+)\pi^+\pi^+\pi^-(+\text{c.c.})$, mode [5, 7] which has a factor of two larger branching ratio (0.051$\pm$0.003) but a larger combinatorial background. There are also data on D_s [9] and D^0 mesons [2, 10]. Another window to study open charm is the identification of e^- coming from semileptonic decays [11]. This approach profits from the large branching fraction $f(\bar{c} \to e^-) = 0.095 \pm 0.009$.

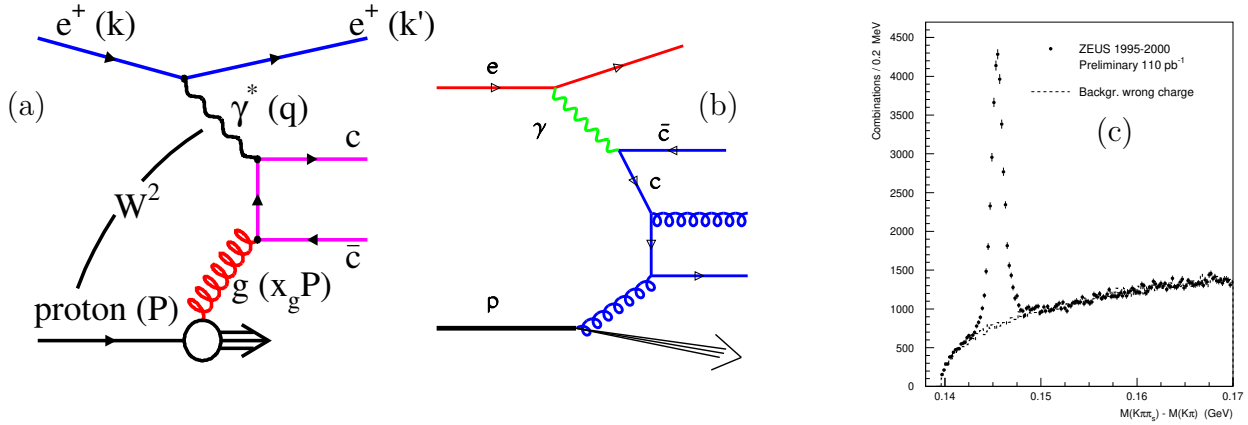

Figure 1. (a) Sketch of the PGF process and (b) charm excitation diagram. (c) D^* peak from [1].

2. Open charm photoproduction

Real photon (γ)-p interactions have a hadronic component in which the γ fluctuates into a hadronic final state (resolved). Thus, factorization has to be applied also for the γ and pdf's have to be measured. In addition to the direct PGF component, a large resolved contribution comes from the " charm excitation" process, Figure 1 (b).

The ZEUS Collaboration [5] has measured the $x_\gamma^{OBS} = \Sigma_{jets} E_T e^{-\eta}/(2yE_e)$ distribution using D^* dijets. The separation between resolved and direct is unique at LO, becoming scheme dependent at NLO. The comparison of the ZEUS data with the HERWIG LO predictions, Figure 2 (a), yields $\sim$ 40% resolved component in the kinematic region of the measurement, dominated by charm excitation. Figure 2 (b) displays the comparison of the dijet data with a massive NLO pQCD prediction produced by the FMNR program [12], which underestimates the low x_γ^{OBS} values (resolved). In the massive approach only light quarks and the gluon pdf's are present in the p and the γ. Another approach is to neglect the mass of the charm quark [13] and treat it as a massless quark. The resummation of logs in $p_{\rm T}/m_c$ results in a charm pdf. The main questions in open charm photoproduction are what is the relative weight of the available production mechanisms and what is the more appropriate model in the HERA range,

massive or massless. However two caveats limit the precision of the test: It is known that the γ pdf's, obtained from fits to F_2^γ, are poorly known in the HERA region and a new iteration including PHP HERA data would be very welcome. Moreover, pQCD cannot predict the fragmentation from a charm quark into a hadron. Thus hadron fractions and fragmentation functions are taken from e^+e^- processes. The Peterson fragmentation function [14], $P(z) \propto z^{-1}[1-1/z-\epsilon/(1-z)]^{-2}$ is convoluted with the charm quark distribution produced by the partonic matrix element, scaling the momentum of the charm quark to that of the D^* meson by z. Note that this model is not Lorentz invariant because of the masses involved. $f(c \to D^{*+}) = 0.235 \pm 0.007 \pm 0.007$ [15] and $\epsilon = 0.035$ [16] are typically used for D^* cross section predictions.

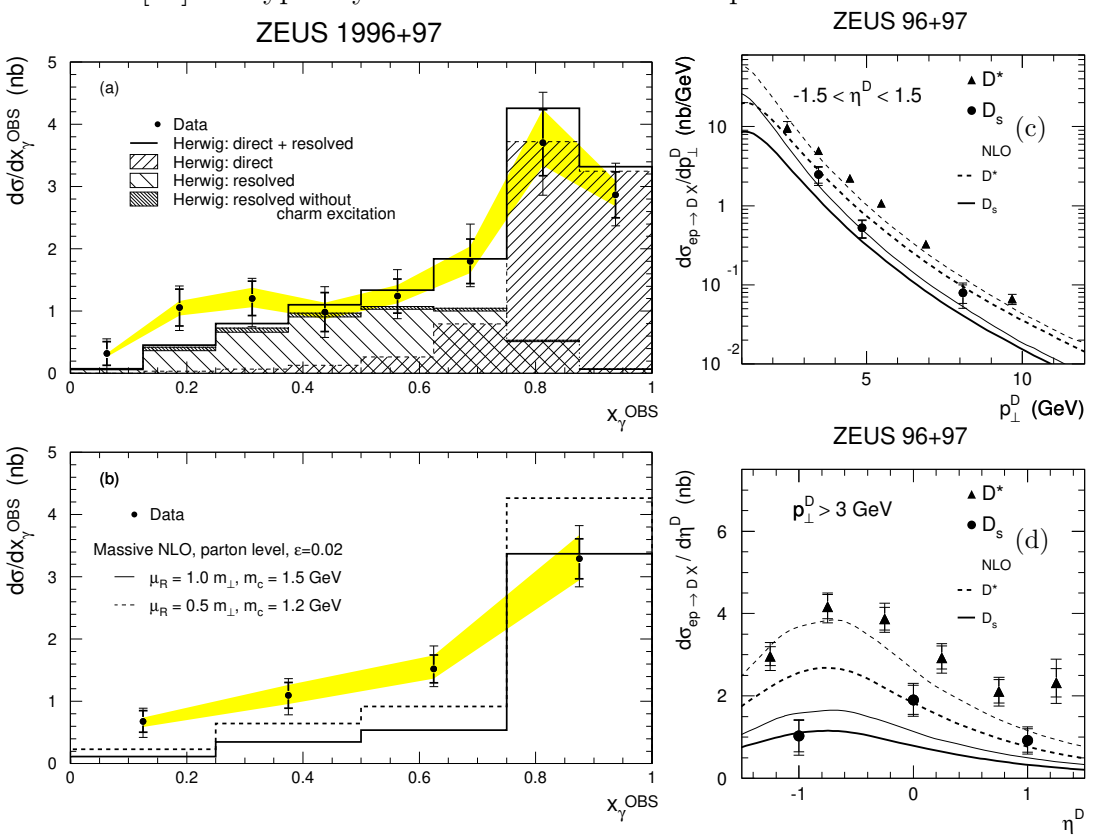

Figure 2. Untagged PHP D^* dijet cross section differential in x_γ^{OBS} compared to HERWIG (a) and FMNR (b). Inclusive D meson differential cross sections $d\sigma/dp_\perp^D$ (c) and $d\sigma/d\eta^D$ (d) where D stands for D_s (dots) and D^* (triangles). Thick (thin) curves in (b) (c) (d) are FMNR predictions with parameters set to $m_c = 1.5(1.2)$ GeV, $\mu_R = \sqrt{m_c^2 + p_T^2}(0.5\sqrt{m_c^2 + p_T^2})$ and $\mu_F = 2(4)\mu_R$.

ZEUS has measured D^* [5] and D_s [9] untagged PHP, where the scattered lepton escapes undetected through the beam hole, using 38 pb^{-1} of $\sqrt{s} = 300$ GeV data. The kinematic region of the untagged measurements is: $130 < W < 280$ GeV, $Q^2 < 1$ GeV^2 ($Q^2_{\rm median} \approx 3 \cdot 10^{-4}$ GeV^2). The D_s mesons are reconstructed using the $D_s^+ \to \phi\pi^+ \to (K^+K^-)\pi^+(+c.c.)$ channel. Experimental restrictions result in the phase space limitation $3 < p_T(D_s) < 12$ GeV and $|\,\eta(D_s)\,| < 1.5$.

The fraction of the D_s to the D^* cross sections in the above phase space region

is measured to be $\frac{\sigma(D_s)}{\sigma(D^*)} = 0.41 \pm 0.07(stat.)^{+0.03}_{-0.05}(syst.) \pm 0.10(br.)$. This quantity is sensitive within the string model to the strange suppression parameter, γ_s. With the help of JETSET, $\gamma_s = 0.27 \pm 0.05 \pm 0.07(br.)$ is obtained. This is in agreement with e^+e^- and therefore supports the universality of c fragmentation found in the earlier H1 publication [2] and the more recent ZEUS results [10, 17].

Figures 2 (c) and (d) display differential cross sections of D_s and D^* in untagged PHP. Most of the branching ratio error, which dominates the γ_s measurement, can be neglected in the comparison with the calculation since it scales the data and the prediction in the same way. The curves are the FO NLO pQCD prediction from FMNR using MRSG (p, α_s=0.114) and GRV-G HO (γ, α_s=0.111) pdf's and the Peterson fragmentation parameter ϵ=0.035. Normalization uncertainties coming from the luminosity measurement (1.7%) and the hadronization fractions (3% for $D^*$and 9% for D_s) are not plotted. The D_s data support the conclusions of the more accurate D^* data, namely:

- The normalization of the theory is too low.
- The shape of the η distribution is not well described.

Massless predictions give a better description of the data both in shape and normalization as can be seen in Figure 3. The parameters for the calculation are pdf CTEQ4M (p, $\alpha_s = 0.116$), $\epsilon = 0.1$, $\mu_R = \sqrt{m_c^2 + p_T^2}$; $m_c = 1.5$ GeV ; $\mu_F = 2\mu_R$. The different curves are due to different γ pdf's. Surprisingly enough, the predictions using GS-G HO, with a charm pdf equal to the up pdf, are closest to the data. The better agreement of the massless calculations is not expected since resummation effects are small for $p_{\rm T}(D^*)$<10 GeV, i.e. in the region of the measurement [18].

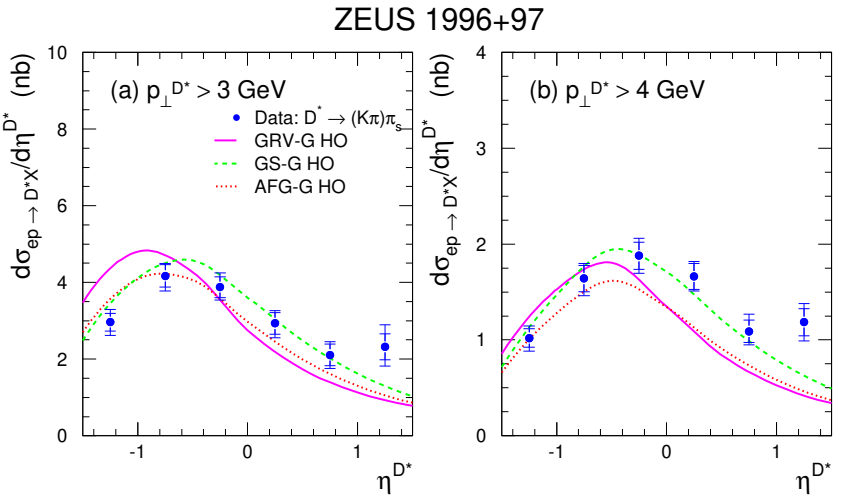

Figure 3. Untagged PHP differential cross sections $d\sigma/d\eta^{D^*}$ compared to massless NLO calculations (see text) using different γ pdf's.

ZEUS has also measured tagged PHP [6] yielding a similar level of description by FMNR. These data are better described by the BKL model [19], which fits the untagged sample.

The H1 Collaboration has measured open charm PHP selected using the 44 (*33*) m taggers [3]. The kinematic region of the measurement is: $Q^2 < 0.009(0.01)\text{GeV}^2$,

$< W >= 88(194)$ GeV, $p_T(D^*) > 2(2.5)$ GeV and | rapidity(D^*) |< 1.5. The data are compared in Figure 4 with the FMNR prediction using pdf's MRST1 (p, α_s=0.1175), GRV-HO (γ), $\epsilon = 0.035$, $\mu_R = \sqrt{m_c^2 + p_T^2}$; $m_c = 1.3 - 1.7$ GeV ; $\mu_F = 2\mu_R$. This calculations used an old value of $f(c \to D^*)$, 15% higher than the latest result (0.235). Also the use of a larger value of α_s than in the case of the ZEUS analysis produces higher values of the prediction. The H1 Collaboration finds good agreement with FMNR and uses this calculation to extract $x_g g(x_g)$.

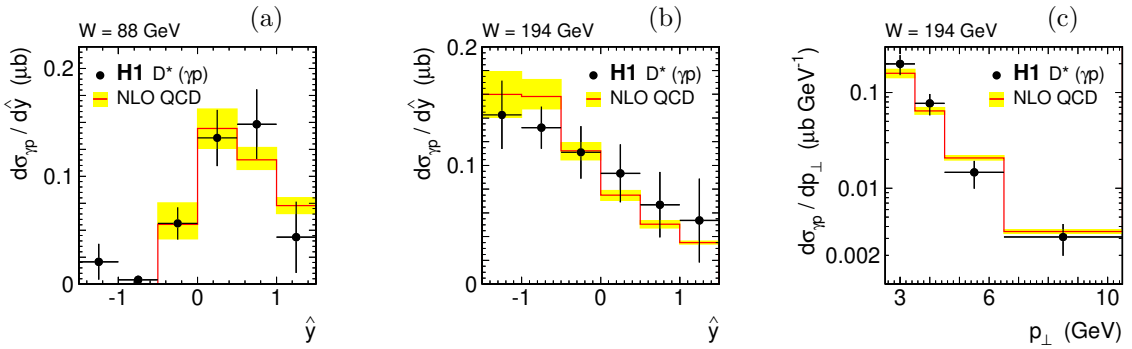

Figure 4. Tagged PHP D^* cross section differential in rapidity (a) (b) and $p_{\rm T}$ (c).

3. Open charm electroproduction

Earlier HERA ($\sqrt{s} = 300$ GeV) and fixed target data ($\sqrt{s} \sim 30$ GeV) show that open charm electroproduction is dominated by PGF, thus providing direct sensitivity to the gluon pdf in the p. FO NLO pQCD calculations are available in the form of a MC integrator (HVQDIS) [20]. Only light quarks and the gluon are present in the p concerning the pdf's. Since open charm electroproduction is sensitive to the gluon, this process allows a test of factorization and in particular of the universality of the gluon pdf, comparing the data with NLO predictions which use as an input the pdf's obtained from fits to inclusive F_2. The same fragmentation limitations mentioned before for PHP apply here.

ZEUS has measured D^* production in DIS using $\mathcal{L} \sim 37$ pb^{-1} at $\sqrt{s} = 300$ GeV in the kinematic region $1 < Q^2 < 600$ GeV^2, $0.02 < y < 0.7$, $1.5(2.5) < p_T(D^*) < 15$ GeV and | $\eta(D^*)$ |<1.5 [7]. The differential cross sections are shown in Figure 5. The two decays used, $D^* \to K2\pi(K4\pi)$, are in agreement as can be seen in the $p_{\rm T}(D^*)$ distribution. The settings of the NLO HVQDIS prediction are: pdf ZEUS NLO fit (α_s=0.119), $\epsilon = 0.035$ (in the lab), $\mu_R = \mu_F = \sqrt{4m_c^2 + Q^2}$, $m_c = 1.3 - 1.5$ GeV. An old value of $f(c \to D^{*+})$, 9 % lower than the latest result (0.235), was used. The comparison of the data with this prediction (open band) yields the following observations:

- Good agreement with HVQDIS in Q^2, x_{Bj} and W.
- HVQDIS is shifted with respect to the data in the $\eta(D^*)$, $x(D^*)$ distributions.

However, the shaded band, obtained by folding JETSET and the same NLO calculation, describes the data better. The NLO calculation is folded with JETSET by means of reweighting the $pt(c)$,$\eta(c)$ two dimensional distribution of a LO MC after the hard

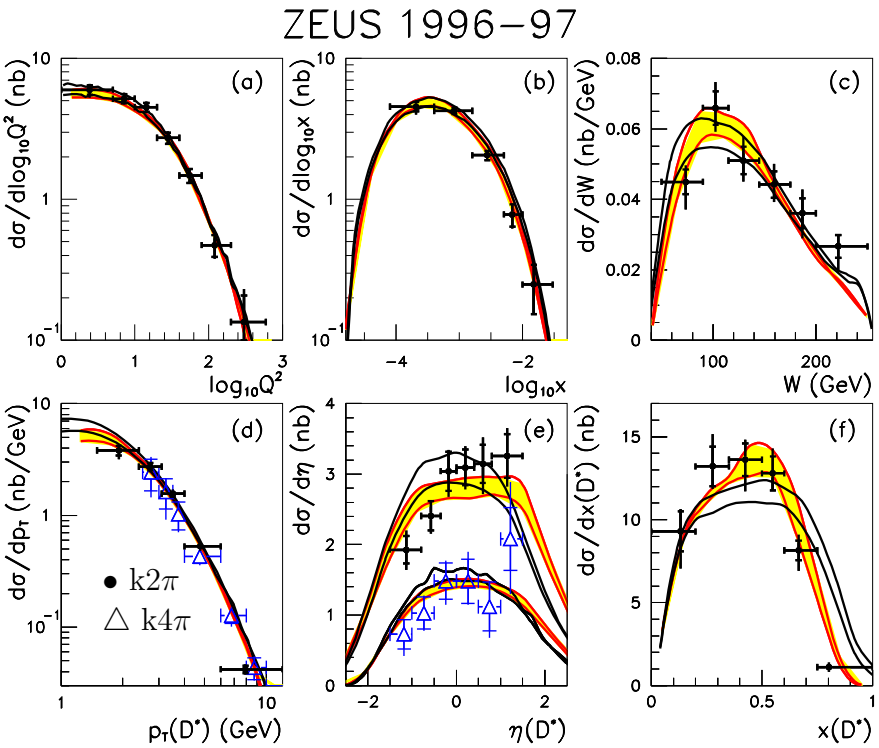

Figure 5. Differential cross sections for D^* production from the $K2\pi$ final state (solid dots) and from the $K4\pi$ channel (open triangles). The open band corresponds to the standard Peterson fragmentation function. The shaded band shows the NLO reweighted JETSET MC. $x(D^*)$ (f) is defined as $2p^*(D^*)/W$, where p^* is in the γ^*-p CMS frame.

interaction and letting JETSET hadronize. A shift into the forward direction due to the string model is observed. A similar picture is obtained using HERWIG or ARIADNE. Figure 6 shows that the shift in η coming from the full fragmentation model (PS+string model) is similar to the effect coming from the string model alone. This shift is expected in models which include the interaction of the colour charges in the final state since the colour configuration is similar to $e^+e^- \to q\bar{q}g$, where the string effect was observed. In PGF processes the remnant is acting as a colour octet which drags the c, $\bar{c}$ into the forward region.

ZEUS has measured cross sections of e^- coming from semileptonic decays of charm in DIS using $\mathcal{L} \sim 34$ pb^{-1} [11]. This measurement relies on the dE/dx deposition of the tracks in the CTD to separate the e^- signal from the hadronic background. The kinematic region is: $1.2 < p_e < 5$ GeV, $|\,\eta_e\,| < 1.1$, $1 < Q^2 < 1000$ GeV^2, $0.03 < y < 0.7$. The method is complementary to the D^* analysis since, on one hand, it profits from the larger branching fraction by being able to go to higher Q^2 and, on the other hand, it probes harder c quarks, providing a p_T enriched sample. The price to pay is that it covers a smaller region of the c quark phase space. The data are in agreement with NLO HVQDIS (see Figure 7), which in this case uses the settings: pdf GRV94 H0 ($\alpha_s = 0.111$), $\epsilon = 0.035$, $\mu_R = \mu_F = \sqrt{4m_c^2 + Q^2}$ and $m_c = 1.3 - 1.7$ GeV.

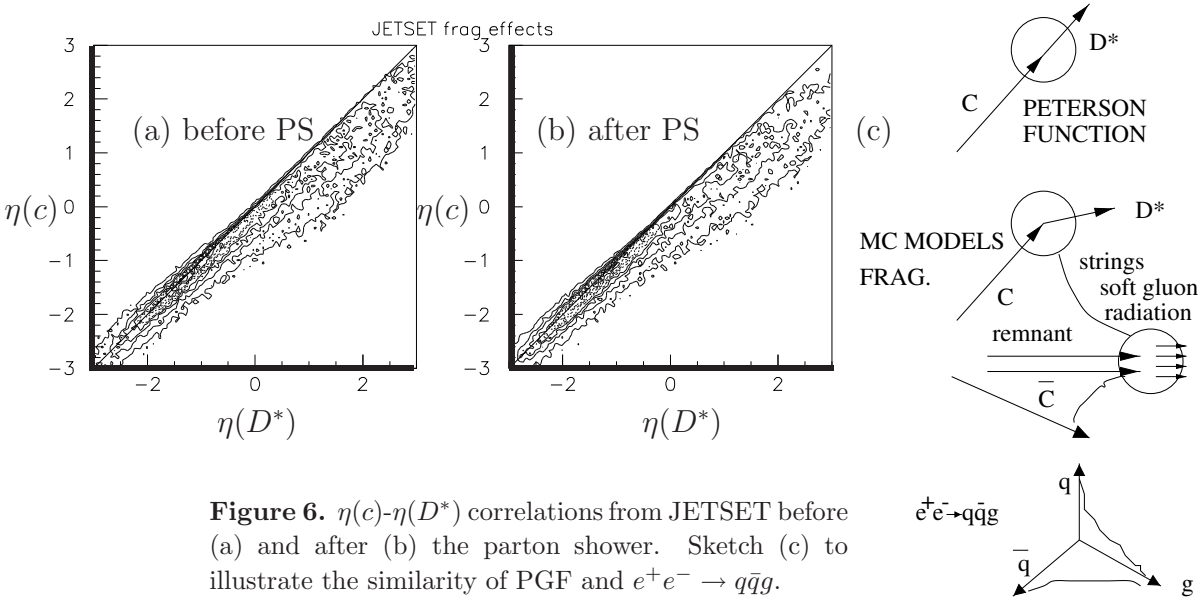

Figure 6. $\eta(c)$-$\eta(D^*)$ correlations from JETSET before (a) and after (b) the parton shower. Sketch (c) to illustrate the similarity of PGF and $e^+e^- \to q\bar{q}g$.

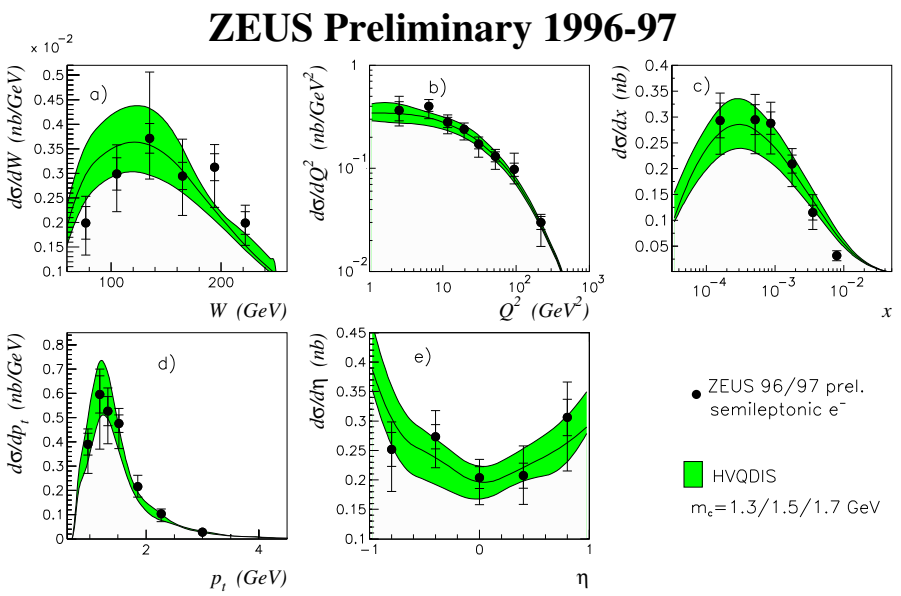

Figure 7. Semileptonic e^- differential cross sections.

ZEUS has also measured D^* production cross sections integrating two samples at different $\sqrt{s}$ with $\mathcal{L}_{\sqrt{s}=300,318} \sim 45,38$ pb^{-1} [8]. The integrated cross section in the kinematic region $10 < Q^2 < 1000$ GeV^2, $0.04 < y < 0.95$, $1.5 < p_T(D^*) < 15$ GeV and $\mid \eta(D^*) \mid < 1.5$ is $\sigma(e^+p \to e^+D^{*\pm}X) = 2.33 \pm 0.12(\text{stat.})^{+0.11}_{-0.07}(\text{syst.})$ nb. This result and the differential cross sections compare reasonably well with NLO HVQDIS using three different pdf's (see Figure 8). Although the measurement limits have been pushed towards high Q^2 and x_{Bj}, MC studies show that there is no sensitivity to intrinsic charm (IC) yet. Another issue in this region is whether variable flavour number schemes (VFNS), which include a charm pdf arising from the resummation of large $log(Q^2/m_c)$

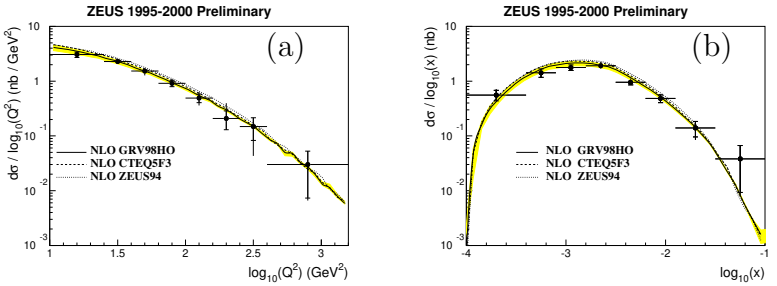

pdf	Λ^4_{QCD} (MeV)	σ(nb) m_c=1.3-1.6
GRV98	257	2.71-2.27
CTEQF53	326	2.95-2.48
ZEUS NLO	404	3.2-2.63

Figure 8. D^* cross sections differential in $log_{10}(Q^2)$ (a) and $log_{10}(x_{Bj})$ (b).

can give a better description of the data than that of the FO NLO pQCD predictions. Little difference between FFNS and VFNS's was found in [21] until $x_{Bj} > 0.1$ and high Q^2. However, a slight difference appears at $Q^2 \sim 10$ GeV^2, Figure 9. Even if the effect is not an artifact introduced by the use of HVQDIS to produce VFNS predictions differential in the c phase space or by the normalization of all curves at $Q^2 = m_c^2$, the question is whether it can be distinguished from fragmentation and/or mass uncertainties which are of the same order.

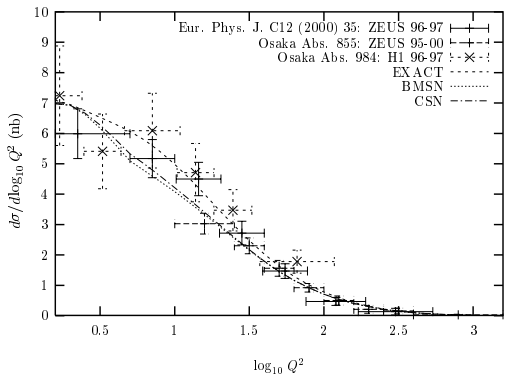

Figure 9. FO NLO pQCD (labeled Exact) is compared with two VFNS predictions and with H1 and ZEUS data. Figure taken from [21].

The H1 Collaboration has performed a measurement of D^* production in DIS using $\mathcal{L} \sim 18$ pb^{-1} [4]. The integrated cross section in the kinematic region $1 < Q^2 < 100$ GeV^2, $0.05 < y < 0.7$, $1.5\ GeV < p_T(D^*)$ and $|\ \eta(D^*)\ | < 1.5$ is: $\sigma_{KIN}(e^+p \rightarrow e^+D^{*\pm}X) = 8.50 \pm 0.42(\text{stat.})^{+1.02}_{-0.76}(\text{syst.}) \pm 0.65(\text{mod.})$ nb. This can be directly compared with the ZEUS measurement [7] in the similar kinematic region $1 < Q^2 < 600$ GeV^2, $0.02 < y < 0.7$, $1.5 < p_T(D^*) < 15$ GeV, $|\ \eta(D^*)\ | < 1.5$: $\sigma_{KIN}(e^+p \rightarrow e^+D^{*\pm}X) = 8.31 \pm 0.31(\text{stat.})^{+0.3}_{-0.5}(\text{syst.})$ nb using HVQDIS to interpolate between the two measurements.

$$R_{KIN} = \frac{\sigma^{HVQDIS}_{ZEUSKIN}}{\sigma^{HVQDIS}_{H1KIN}} = 1.11 \quad \Rightarrow \quad \frac{R^{DATA}_{KIN}}{R^{HVQDIS}_{KIN}} = 0.88^{+0.12}_{-0.15}, \tag{2}$$

which is compatible with 1. This, and the comparison of the differential cross sections in $log_{10}(Q^2)$, see Figure 9, support the fact that H1 and ZEUS data agree within errors.

H1's data are compared with HVQDIS using pdf GRV98 (α_s=0.114), m_c=1.3-1.5 GeV. In addition to the standard Peterson ϵ=0.035-0.1 (in γ^*p CMS), a transverse momentum with respect to the charm quark is given to the D^* meson, according to the

function $exp(-\alpha p_t^2)$ with $< p_t^2 > \approx$350 MeV. This results in a prediction for the cross section of $7.02 - 5.17$ nb. The H1 analysis also compares the data with CASCADE [22], which implements the CCFM evolution. In this model an unintegrated gluon density, fitted to H1's F_2, and m_c=1.3-1.5 GeV are used. The fragmentation is performed by JETSET with ϵ=0.035-0.1 yielding $10.77 - 8.04$ nb. The measured single and double differential cross sections are compared to these calculations in Figure 10. CASCADE shows better agreement in normalization, while the HVQDIS prediction is too low at forward η, low z_{D^*} (Figures 10 (e) and (f)). The double differential cross section (Figure 10 (g)) shows that the disagreement with HVQDIS is concentrated at low $p_{\rm T}(D^*)$ and forward $\eta(D^*)$, which is correlated with low z_{D^*}. Moreover there is a poor agreement with CASCADE at high $p_{\rm T}(D^*)$.

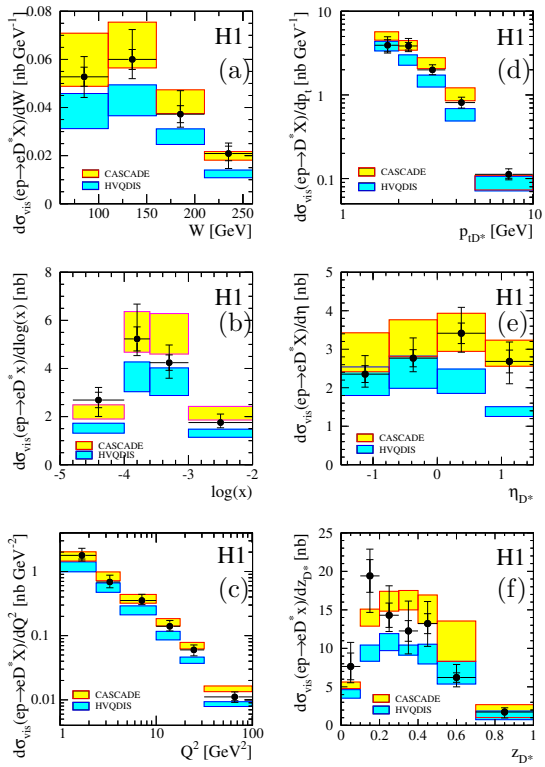

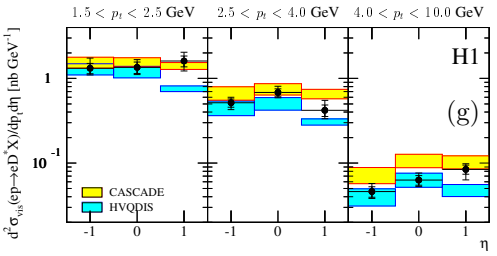

Figure 10. Differential D^* cross sections vs W (a), x_{Bj} (b), Q^2 (c), $p_{\rm T}(D^*)$ (d), $\eta(D^*)$ (e), $z_{D^*} = (E-P_z)^{D^*}/(E-P_z)^{\gamma^*}$ (f) compared with HVQDIS and CASCADE predictions (see text). Double differential cross section in $p_{\rm T}(D^*)$ and $\eta(D^*)$ (g) compared with the same calculations.

3.1. Extraction of $F_2^{c\bar{c}}$

$F_2^{c\bar{c}}$ can be defined in terms of the double differential cross section integrating over the full c quark phase space: $\frac{d^2\sigma^{c\bar{c}}(x,Q^2)}{dxdQ^2} = \frac{2\pi\alpha^2}{xQ^4}\{[1+(1-y)^2]F_2^{c\bar{c}}(x,Q^2) - y^2 F_L^{c\bar{c}}\}$. Several assumptions are made in the extraction:

- The contribution of $F_L^{c\bar{c}}$ ($< 1\%$, according to the FO NLO calculations) is neglected.
- Bound charm (<2.5-4.5 % [7]) is neglected.
- $f(c \to D^{*+})$ from e^+e^- is valid at HERA.
- The extrapolation factors, $\frac{\sigma_{INT}}{\sigma_{KIN}}$, are well described by the model used to extrapolate.

The relevance of the last assumption is illustrated by the size of the extrapolation factors, which go from $\leq$2 at high Q^2 to $\leq$4 at low Q^2 for D^* data and can be as large as $\leq$20 at

low Q^2 for e^- data. The actually applied procedure to extrapolate outside the observed kinematic region (KIN) in $p_{\rm T}, \eta$ is:

$$F_{2\ meas}^{c\bar{c}}(Q^2, x_{Bj}) = F_{2\ theo}^{c\bar{c}}(Q^2, x_{Bj}) \times \frac{\sigma_{KIN}^{meas}(Q^2, y)}{\sigma_{KIN}^{theo}(Q^2, y)} \tag{3}$$

The extrapolation is not strongly affected by the fragmentation models because the procedure is not very sensitive to the shape of the η distribution. The information contained in the $F_2^{c\bar{c}}$ plots in Figure 11 can be classified according to its dependence on the extrapolation:

(i) Since $F_{2\ meas}^{c\bar{c}}/F_{2\ theo}^{c\bar{c}} = \sigma_{KIN}^{meas}/\sigma_{KIN}^{theo}$ by construction (see eq. 3), the comparison of $F_{2\ meas}^{c\bar{c}}$ with the $F_{2\ theo}^{c\bar{c}}$ that was used to extrapolate represents the level of agreement at the cross section level and is independent of the extrapolation. The semileptonic double differential cross section $\sigma_{KIN}^{meas}(Q^2, x_{Bj})$ is well described by HVQDIS (GRV94) as can be seen in Figure 11 (a). The same is true for the D^* data and HVQDIS (ZEUSNLO), Figure 11 (b). On the other hand, good agreement is observed between the unextrapolated H1 data and CASCADE, Figure 11 (c).

(ii) Statements about the shape of $F_{2\ meas}^{c\bar{c}}$ are model dependent: $F_2^{c\bar{c}}$ rises steeply as x_{Bj} decreases and, when plotted vs. Q^2 at constant x_{Bj} [7], does not scale in the measured region. This can be interpreted as coming from the rise of the gluon via the PGF dominance of open charm electroproduction. $F_2^{c\bar{c}}$ represents $\sim 25{-}30\%$ of F_2 for $Q^2 > 11$ GeV^2 and low x_{Bj}. Figure 11 (b) has two regimes: it flattens at low x_{Bj}, where both $F_2^{c\bar{c}}$ and F_2 are dominated by PGF and, neglecting all mass effects, $F_2^{c\bar{c}}/F_2 \sim \frac{q_c^2}{q_u^2+q_d^2+q_s^2+q_c^2+q_b^2} \sim 4/11 \sim 0.36$. The denominator of the ratio, F_2, rises at high x_{Bj} due to the valence contribution, forcing the ratio to drop.

(iii) Comparing the shape of $F_{2\ meas}^{c\bar{c}}$ with other models, or two $F_{2\ meas}^{c\bar{c}}$ extracted assuming different theories is, to a large extent, a comparison between two models, rather than with data. Of this kind are all comparisons that can be made in Figure 11 (d): $F_{2\ meas}^{c\bar{c}}$ from three independent samples extracted with HVQDIS (GRV 98, GRV 94, ZEUS NLO) seem to be compatible. The prediction using the H1 fit agrees reasonably well with the shape of HVQDIS (GRV 98, GRV 94, ZEUS NLO).

4. Summary

The overall picture is that of reasonable agreement among all data samples, obscured by the different interpretations of these data, especially concerning the level of description by FO NLO pQCD calculations.

In PHP, H1 observes an adequate description by FMNR and uses these data to extract $x_g g(x_g)$. However, ZEUS observes a deficit in the FMNR prediction, specially in the forward region. Alternative models/explanations are massless calculations, BKL, fragmentation effects or large NNLO corrections.

The agreement within theoretical uncertainties of the FO NLO pQCD HVQDIS predictions using pdf's extracted from DGLAP fits to the inclusive F_2 scaling violations

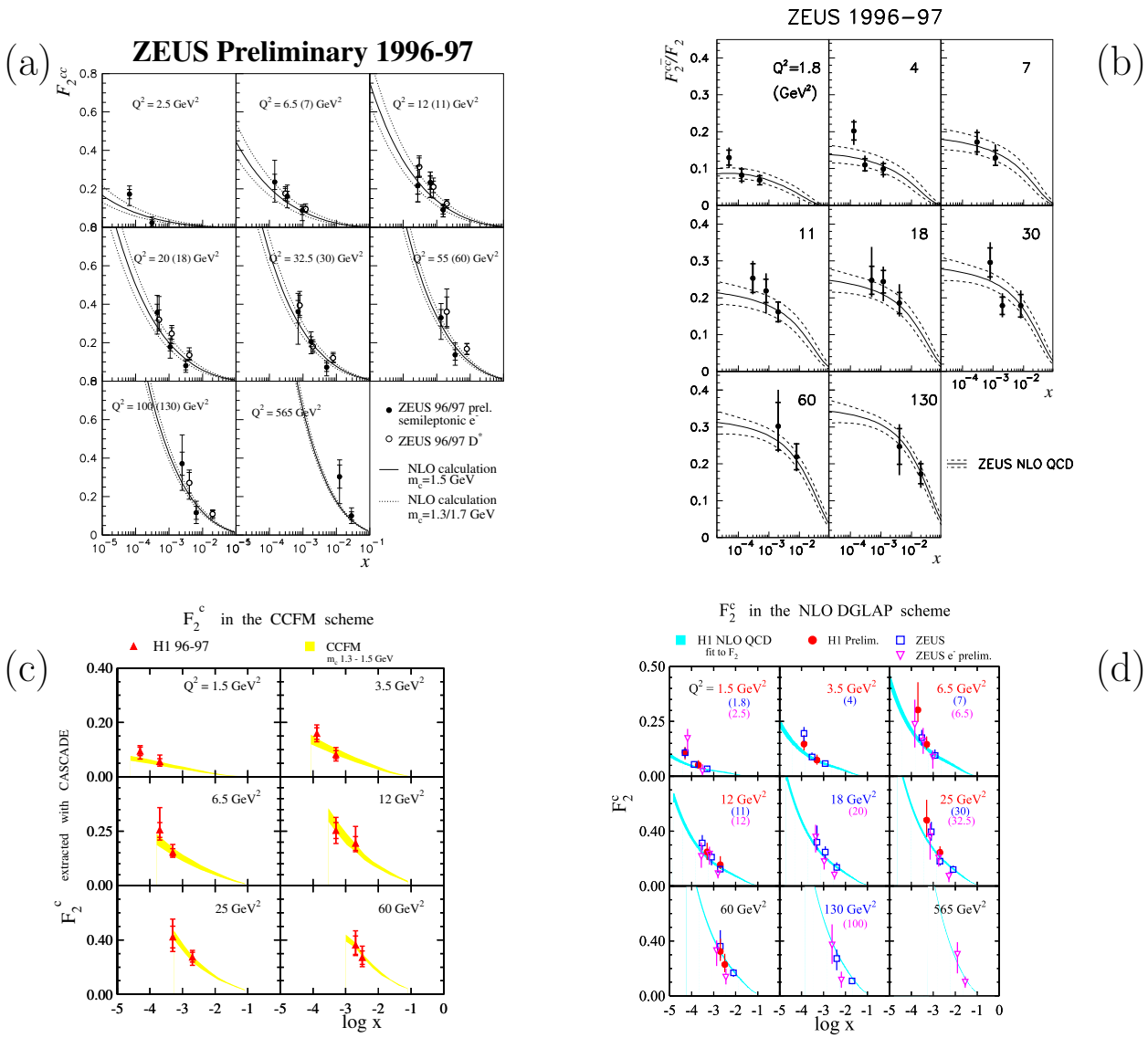

Figure 11. Measured $F_2^{c\bar{c}}$ from semileptonic data [11] vs. x_{Bj} at fixed Q^2 values (a) compared to the model used for the extrapolation (HVQDIS, GRV94). Ratio of the measured $F_2^{c\bar{c}}$ from D^* data [7] extrapolated with (HVQDIS, ZEUSNLO) over F_2 vs. x_{Bj} at fixed Q^2 values (b). Measured $F_2^{c\bar{c}}$ from D^* data [4] vs. x_{Bj} at fixed Q^2 values compared to the model used for the extrapolation (CASCADE) (c). The data of (a) and (b) compared with the H1 data [4] extracted with HVQDIS,GRV98 (d).

with the H1 and ZEUS D^* production cross section and the ZEUS semileptonic cross section provides support for the universality of the parton distributions of the p and the validity of factorization in charm electroproduction. However, H1 finds better agreement with CASCADE predictions than with those of HVQDIS.

5. Outlook

Measurements of open charm production will benefit from the expected increase of a factor of 5 in luminosity, together with the instrumental improvements of the H1 and ZEUS detectors in HERA Run II. This can result in an extended coverage of the phase

space, especially in the forward region, which could be used to:

- Improve the understanding of charm photoproduction.
- Increase the sensitivity to intrinsic charm in DIS, since forward η correspond to higher x_{Bj}.
- Look for indications to distinguish between the VFNS approach and FO NLO.
- Minimize the extrapolation dependence of $F_2^{c\bar{c}}$. In this case it would be useful to explore channels beyond the usual D^* modes, whose lower p_{T} limit is fixed because of the good correlation between $p_{\mathrm{T}}(D^*)$ and $p_{\mathrm{T}}(\pi_s)$.

Ongoing studies on c-meson spectroscopy [1, 10, 17], diffraction [23] or double tagged final states will also benefit from the increase in statistics.

On the theoretical side, an improved treatment of fragmentation, matching the NLO calculation to MC fragmentation models such as JETSET, could lead to a better description of the data. It would be also desirable to identify a more distinctive signature for CCFM evolution. The final goal is to include open charm cross section data in global pdf fits.

Acknowledgements

I thank the organizers of the Ringberg Workshop for the nice atmosphere. The author is financially supported by the Comunidad Autónoma de Madrid.

References

[1] Breitweg J *et al* [ZEUS Collaboration] 2000, Contributed paper to XXXth ICHEP, abstract 854.
[2] Adloff C *et al* [H1 Collaboration] 1996, *Z. Phys.* C**72**, 593.
[3] Adloff C *et al* [H1 Collaboration] 1999, *Nucl. Phys.* B **545**, 21.
[4] Adloff C *et al* [H1 Collaboration] 2000, Contributed paper to XXXth ICHEP, abstract 984. Mohrdieck S [H1 Collaboration], talk at DIS2001, http://dis2001.bo.infn.it/wg/sfwg.html.
[5] Breitweg J *et al* [ZEUS Collaboration] 1999, *Eur. Phys. J.* C **6**, 67.
[6] Breitweg J *et al* [ZEUS Collaboration] 1999, Contributed paper to XXIXth EPS, abstract 525.
[7] Breitweg J *et al* [ZEUS Collaboration] 2000, *Eur. Phys. J.* C **12** 1, 35.
[8] Breitweg J *et al* [ZEUS Collaboration] 2000, Contributed paper to XXXth ICHEP, abstract 855.
[9] Breitweg J *et al* [ZEUS Collaboration] 2000, *Phys. Lett.* B **481 2-4**, 213.
[10] Chekanov S *et al* [ZEUS Collaboration] 2001, Contributed paper to XXXth EPS, abstract 501.
[11] Breitweg J *et al* [ZEUS Collaboration] 2000, Contributed paper to XXXth ICHEP, abstract 853.
[12] Frixione S, Nason P and Ridolfi G 1995, *Nucl. Phys.* B **454**, 3.
[13] Kniehl B A *et al* 1997, *Z. Phys.* C **76**, 689; Binnewies J *et al* 1997, *Z. Phys.* C **76**, 677; Cacciari M *et al* 1997, *Phys. Lett.* D **55**, 2736.
[14] Peterson C *et al* 1983, *Phys. Rev.* D**27**, 105.
[15] Gladilin L, hep-ex/9912064.
[16] Nason P and Oleari C 2000, *Nucl. Phys.* B **565**, 245.
[17] Chekanov S *et al* [ZEUS Collaboration] 2001, Contributed paper to XXXth EPS, abstract 497.
[18] Frixione S 2001, talk at DIS2001, http://dis2001.bo.infn.it/wg/hiwg.html.
[19] A.V.Berezhnoy, V.V.Kiselev and A.K.Likhoded, hep-ph/990555
[20] Harris B W and Smith J 1998 , *Phys. Rev.* D **57** (1998), 2806; Laenen E, Riemersma S, Smith J and Van Neerven W L 1995, *Nucl. Phys.* B**392**,162.
[21] Chuvakin A , Smith J and Harris B W 2001, *Eur. Phys. J.* C **18**, 547.

[22] Jung H 1999, HERAMC Workshop DESY-PROC-1999-02, 75
[23] Breitweg J *et al* [ZEUS Collaboration] 2000, Contributed paper to XXXth ICHEP, abstract 874.